

# Velocity fluctuations in a low-Reynolds-number fluidized bed

SHANG-YOU TEE<sup>1,2</sup>, P. J. MUCHA<sup>3</sup>, M. P. BRENNER<sup>2</sup>  
AND D. A. WEITZ<sup>1,2</sup>

<sup>1</sup>Department of Physics, Harvard University, Cambridge, MA 02138, USA

<sup>2</sup>School of Engineering and Applied Science, Harvard University, Cambridge, MA 02138, USA

<sup>3</sup>Department of Mathematics & Institute for Advanced Materials,  
University of North Carolina, Chapel Hill, NC 27599, USA

(Received 6 August 2007 and in revised form 18 October 2007)

The velocity fluctuations of particles in a low-Reynolds-number fluidized bed have important similarities and differences with the velocity fluctuations in a low-Reynolds-number sedimenting suspension. We show that, like sedimentation, the velocity fluctuations in a fluidized bed are described well by the balance between density fluctuations due to Poisson statistics and Stokes drag. However, unlike sedimentation, the correlation length of the fluctuations in a fluidized bed increases with volume fraction. We argue that this difference arises because the relaxation time of density fluctuations is completely different in the two systems.

---

A flurry of recent work has focused on understanding velocity fluctuations in a suspension of particles sedimenting due to gravity (Asmolov 2004; Bargiel, Ford & Tory 2005; Bergougnoux *et al.* 2003; Cunha *et al.* 2002*a*; Cunha, Sousa & Hinch 2002*b*; Kuusela, Lahtinen & Ala-Nissila 2003, 2004; Mucha & Brenner 2003; Mucha *et al.* 2004; Nguyen & Ladd 2005; Tee *et al.* 2002). When the system-size Reynolds number,  $Re$ , is low and the particle Péclet number,  $Pe$ , is high, both inertial and thermal effects are negligible, and hydrodynamic interactions lead to highly complex behavior that has defied complete explanation. Early theoretical work argued that in a fully mixed system, velocity fluctuations arise from the balance between Stokes drag and density fluctuations in the particle distribution due to Poisson statistics (Caflisch & Luke 1985; Hinch 1988). Thus, a region of size  $l$  has a typical particle number fluctuation of  $\Delta N \approx \sqrt{N} = \sqrt{\phi l^3/a^3}$ , resulting in a buoyant weight of  $\Delta N \frac{4}{3}\pi a^3 \Delta \rho g$ , which must be balanced by its Stokes drag,  $6\pi\eta l \Delta v$ ; this leads to a typical velocity fluctuation of  $\Delta v \sim \sqrt{\phi l/a}$ . Here,  $\phi$  is the volume fraction,  $a$  the particle radius,  $\Delta \rho$  the density difference between particle and fluid,  $g$  the gravitational acceleration, and  $\eta$  the fluid viscosity. This implies that velocity fluctuations should be dominated by density fluctuations on the scale of the system,  $d$ , and hence should diverge with  $d$  (Caflisch & Luke 1985; Hinch 1988); however this contradicts experimental observations (Ham & Homsy 1988; Nicolai & Guazzelli 1995; Segrè, Herbolzheimer & Chaikin 1997). Nevertheless, this theoretical argument does correctly predict velocity fluctuations up to the correlation length,  $\xi$ , to which density fluctuations persist. Much controversy has surrounded the mechanism for keeping this length scale of the density fluctuations smaller than  $d$ . Recently, it has become apparent that system inhomogeneities such as stratification (Mucha *et al.* 2004; Tee *et al.* 2002) or particle-size polydispersity (Bergougnoux *et al.* 2003) can limit the scale of  $\xi$ .

In a fluidized bed, liquid is pumped upwards to exactly counteract particle sedimentation, allowing it to achieve a statistically steady state (Cowan, Page & Weitz 2000; Martin, Rakotomalala & Salin 1995; Segrè 2002; Segrè & McClymer 2004). Nevertheless, long-ranged hydrodynamic interactions between particles create velocity fluctuations which have been assumed identical to those of sedimentation (Cowan *et al.* 2000; Martin *et al.* 1995; Page, Cowan & Weitz 2000; Segrè 2002; Segrè & McClymer 2004; Xue *et al.* 1992). Indeed, the earliest experiments measuring the volume fraction dependence of the hydrodynamic dispersion coefficient were carried out in a fluidized bed, showing an increase with particle volume fraction (Martin *et al.* 1995). The introduction of particle image velocimetry to both sedimentation (Guazzelli 2001; Segrè *et al.* 1997, 2001; Tee *et al.* 2002) and fluidized beds (Segrè 2002; Segrè & McClymer 2004) demonstrates that the fluctuations in the two experiments are visually quite similar.

Are the velocity fluctuations in a fluidized bed controlled by the same mechanism as sedimentation? In this paper, we demonstrate that, like sedimentation, the velocity fluctuations in a fluidized bed are governed by the balance of local Poisson density fluctuations and Stokes drag. However, the volume fraction dependence of the velocity fluctuations and the correlation length are strikingly different in the two systems: for example the correlation length increases (decreases) with volume fraction in a fluidized bed (sedimentation). We present quantitative arguments demonstrating that the reason for this difference is that the two systems have completely different mechanisms for relaxing small density fluctuations.

Our fluidized bed consists of glass spheres of density  $2.23 \text{ g cm}^{-3}$  in silicon oil of viscosity  $\eta = 17.9 \text{ cP}$  and density  $0.854 \text{ g cm}^{-3}$ . We use particles with four different average radii, 49.0, 57.6, 68.8 and  $82.5 \mu\text{m}$  with standard deviations of 4.0, 4.8, 6.3,  $7.5 \mu\text{m}$ , respectively, as measured using a microscope and fitting to Gaussian distributions. The fluidized bed has dimensions of  $1.2 \times 5 \times 35 \text{ cm}$ , and is completely immersed in a stirred water bath to control the temperature to  $23.0 \pm 0.1 \text{ }^\circ\text{C}$ . The silicon oil is pumped into the bed and the overflow from the top is recirculated back into the pump, forming a closed loop. Before entering the bed, the oil first passes through a distributor made of packed beads constrained between two pieces of nylon mesh. The fluid at the bed entrance is carefully tested for uniformity and stability by monitoring the motion of tracer particles in the fluid. With the pump turned off, the particles form a sediment at the bottom of the bed. When the pump is turned on, the sediment expands upward to a maximum height,  $h_{max}$ , that depends on the pump velocity,  $v_p$ , defined as the volumetric flow rate divided by the cross-sectional area of the bed. After an initial transient, neither the particle concentration nor fluctuations change in time; thus we assume the particle distribution has reached a statistically steady configuration.

The volume fraction is determined as a function of height,  $h$ , by measuring the transmittance of a laser beam through the fluidized bed with a photodiode, calibrated with known volume fractions of particles. The results are further verified by pipetting known sample volumes from the fluidized bed, and weighing particles after removing the oil to determine  $\phi$ . The particles are index-matched to the fluid, and a small number of coloured tracer particles are added; images of these particles are collected from the mid-plane of the bed with a charged-coupled device (CCD) camera ( $640 \times 480$  pixels), using a lens with a depth of focus of  $\sim 6 \text{ mm}$  and cross-sectional area of  $4 \times 3 \text{ cm}$ . Particle motion is analysed with particle image velocimetry (PIV) (Adrian 1991; Raffel 1998). The interrogation time between two PIV image pairs is chosen such that the in-plane velocity components do not carry the particle more than 20 % of the size

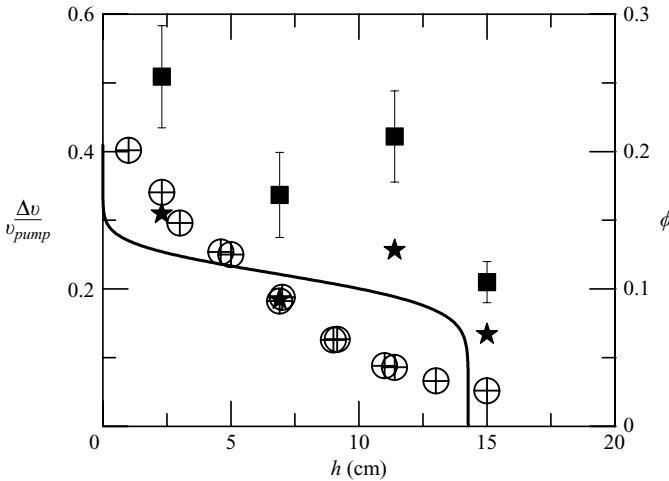


FIGURE 1. Vertical and horizontal velocity fluctuations normalized by pump velocity (square and star symbols, respectively) and volume fraction (hatched symbols) as a function of bed height for spheres of radius  $57.8 \pm 4.8 \mu\text{m}$ . The solid line corresponds to the volume fraction given by a perfectly segregated model. Error bars for the velocity fluctuations are standard deviations of the measurements.

of the interrogation region. The size of the interrogation region is chosen to properly resolve the correlation lengths, and we use regions as small as  $0.5 \times 0.375 \text{ cm}$ . The interrogation times range from about 30 s to 8 min depending on the particle radius, and particle concentrations. We measure the locally coarse-grained particle velocities to verify that there are no convective flows either parallel or perpendicular to the thickness of the bed, in agreement with previous measurements (Segrè 2002; Segrè & McClymer 2004). We determine the vertical-velocity fluctuations,  $\Delta v = \langle v_z^2 \rangle^{1/2}$ , where  $v_z$  is the local vertical component of the velocity.

For weakly spreading and perfectly monodisperse particles,  $\phi$  is expected to be homogeneous throughout the bed (Couderc *et al.* 1985; Martin *et al.* 1995), with a volume fraction set by the Richardson–Zaki (R–Z) relation,  $v_p = v_s(1 - \phi)^{5.5}$ . However, we observe that  $\phi$  exhibits a pronounced dependence on height as illustrated by a suspension of  $7.8 \times 10^6$  particles of radius  $57.8 \pm 4.8 \mu\text{m}$ , with a pump velocity of  $v_p = 0.038 \text{ cm s}^{-1}$ , shown by the hatched circles in figure 1. We hypothesize that this is due to particle size polydispersity; to test this, we use a bidisperse mixture of  $3.3 \times 10^6$  particles with  $a = 68.8 \pm 6.3 \mu\text{m}$  and  $2.4 \times 10^6$  particles with  $a = 82.5 \pm 7.5 \mu\text{m}$ . Consistent with our hypothesis, the  $h$ -dependence is even more pronounced, as shown by the hatched circles in figure 2. To further confirm that this behavior is due to polydispersity, we pipette small samples of particles from near the top and bottom of the bed and measure sizes with a microscope. For both experiments, there is clear segregation of particle sizes, with more larger particles near the bottom of the bed and more smaller particles near the top, as shown in figure 3. The separation is greater in the bidisperse experiment, reflecting the greater tendency of particles to segregate when their size difference becomes more pronounced. The results shown in figures 1–3 are quite reproducible from run to run; repeat runs were conducted by turning off the pump, and waiting for all of the particles to settle before re-fluidizing the bed.

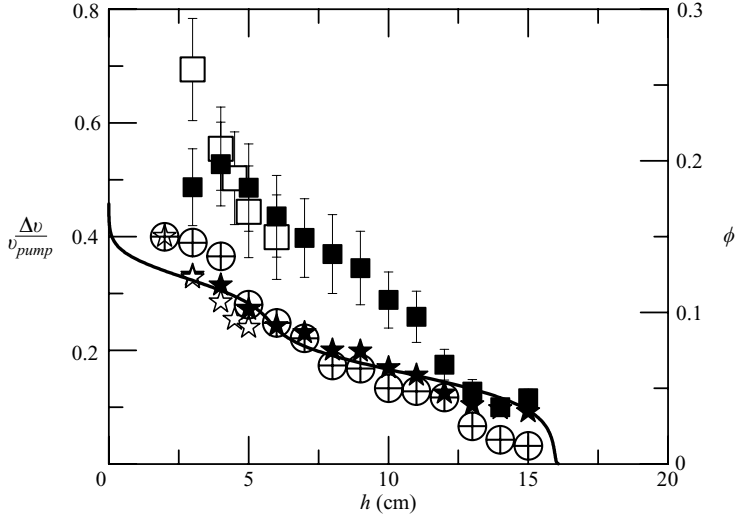


FIGURE 2. Vertical and horizontal velocity fluctuations normalized by pump velocity for spheres of radii  $68.8 \pm 6.3 \mu\text{m}$  (square and star solid symbols) and  $82.5 \pm 7.5 \mu\text{m}$  (square and star open symbols) and combined volume fraction (hatched symbols) as a function of bed height. The solid line is the volume fraction given by a perfectly segregated model. Error bars for the velocity fluctuations are standard deviations of the measurements.

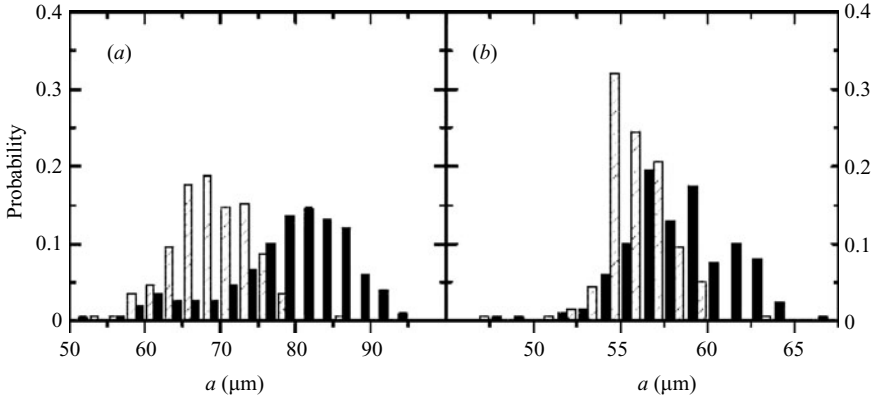


FIGURE 3. Size distributions of particles drawn from two experiments. (a) Particles of sizes  $68.8 \pm 6.3 \mu\text{m}$  and  $82.5 \pm 7.5 \mu\text{m}$ . Particles drawn from the top of the bed, shaded bars ( $h = 15 \text{ cm}$ ), are almost all of size  $68.8 \pm 6.3 \mu\text{m}$  whereas particles drawn from the bottom of the bed, solid bars ( $h = 3 \text{ cm}$ ), have sizes that range from  $62.5$  to  $90 \mu\text{m}$ . (b) Particles of radius  $57.8 \pm 4.8 \mu\text{m}$ . Particles drawn from the top of the bed, shaded bars, ( $h = 15 \text{ cm}$ ) are slightly smaller in size than those drawn from the bottom, solid bars ( $h = 3 \text{ cm}$ ).

That polydispersity can lead to an inhomogeneous fluidized bed follows from classical ideas of Batchelor (Batchelor 1982; Batchelor & Wen 1982), who demonstrated that a particle's sedimentation velocity is slowed by the presence of other particles, due primarily to the settling of a particle being impaired by the backflow of the other particles. Physically, smaller particles near the bottom of the bed are pushed upwards because the interstitial flow of larger particles is faster than the smaller particles' sedimentation velocity in isolation. Indeed, a series of sedimentation experiments (Al-Naafa & Selim 1992; Bruneau *et al.* 1990; Davies 1968; Hoyos

*et al.* 1994; Lockett & Alhabboo 1973; Mirza & Richardson 1979; Selim, Kothari & Turian 1983; Smith 1965, 1966, 1967) have demonstrated that these particle interactions lead to segregation of different particle sizes.

A simple way to test whether the  $h$ -dependence of  $\phi$  is consistent with segregation of the particle sizes is to compute the  $\phi$  profile under the assumption that size segregation is perfect, and that the R-Z relation is valid locally. To numerically calculate the predicted  $h$ -dependence of  $\phi$  with this model, we finely discretize the particle distribution into bins, set the largest particles at the bottom of the bed, stack the next bin of slightly smaller particles above it and continue stacking bins of successively smaller particles until the bin of smallest particles is at the top of the bed. For steady state, we require each of these bins of particles to separately satisfy the R-Z relation. Since larger particles have higher sedimentation velocity  $v_s$ , a bin of larger particles must have a higher  $\phi$ ; likewise, a bin of smaller particles must have a lower  $\phi$ . Using the calculated values  $\phi$  and the cross-sectional area of the bed, the height of each bin is determined. The profile of  $\phi$  converges as the bin size is decreased.

What determines the bed height, as well as the characteristic length scale over which  $\phi$  varies? Qualitatively, the R-Z relation predicts that the bed height and the scale of  $\phi$  variation increase with increased pump velocity. This is because the self-sharpening effect at the suspension–fluid interface becomes stronger as  $\phi$  is increased. Indeed, for the slightly polydisperse particles of  $57.8 \pm 4.8 \mu\text{m}$ , at low pump velocities,  $\phi$  is very high ( $\sim 0.4$  and  $0.5$ ) and almost constant throughout the bed height whereas at high pump velocity,  $\phi$  depends strongly on bed height as in figure 1. Even though this model does not quantitatively agree well with the  $57.8 \pm 4.8 \mu\text{m}$  particles at high flow rate, it shows qualitatively that bed volume fraction profiles become steeper with higher flow rates, in agreement with experiments.

Just as  $\phi$  exhibits a pronounced  $h$  dependence, so too do the velocity fluctuations;  $\Delta v/v_p$  is substantially larger at the bottom of the fluidized bed than at the top, both for the monodisperse particles and for the bidisperse particles, as shown by the solid and open squares in figures 1 and 2. The velocity fluctuations are correlated over length scales,  $\xi$  (Segrè *et al.* 1997); to determine this, we measure the correlation function  $C_z(z) = \langle \Delta v_z(0) \Delta v_z(z) \rangle / \langle \Delta v_z(0)^2 \rangle$  and fit the results to  $C_z(z) = \exp(-z/\xi)$ . We find that  $\xi$  decreases with increasing height, as shown in the inset of figure 4. Physically, we expect that each sphere is advected within a correlated velocity fluctuation, travelling a distance  $\sim \xi$  until the correlation decays in a time,  $\tau \sim \xi v \Delta v$ , whereupon the particle becomes entrained in a new region of correlated fluctuating velocity.

However, note that the low Reynolds number of the fluidized bed implies that there is a steady parabolic flow across the thickness of the bed, with the velocity vanishing on the walls of the cell. This could complicate interpretation of the velocity fluctuations in this system. If we assume the velocity fluctuations are independent of the imposed flow, the measured velocity fluctuations are the sum of that from the parabolic flow and the intrinsic fluctuations:  $\Delta v^2 = \Delta v_{\text{parabolic}}^2 + \Delta v_{\text{fluctuation}}^2$ . For most measurements here  $\Delta v_{\text{parabolic}}^2$  is small compared to  $\Delta v_{\text{fluctuation}}^2$ . With the depth of focus spanning the middle half a cell with parabolic velocity profile peaking at  $V_c = 3v_p/2$  on the centreline, the average velocity in that middle half is  $11V_c/12$ , and the variance about that average is  $\Delta v_{\text{parabolic}}^2 = V_c^2/180 = v_p^2/80$ . This is much smaller than the measured velocity fluctuations.

Any local theory for the velocity fluctuations will predict that the correlation length is driven by variations in  $\phi$ . Thus we plot  $\xi$  as a function of the local  $\phi$ , and find a pronounced dependence, best described as linear, for both monodisperse and bidisperse particles, as shown in figure 4. This differs markedly from sedimentation,

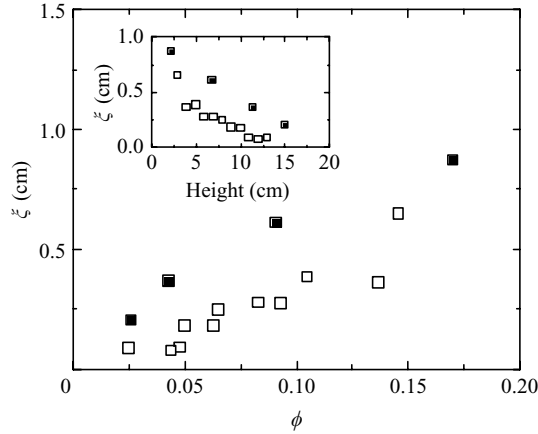


FIGURE 4. Correlation length as a function of volume fraction for a bed fluidized with  $57.8 \pm 4.8 \mu\text{m}$  particles (solid symbols), and with particles of radius  $68.8 \pm 6.3 \mu\text{m}$  and  $82.5 \pm 7.5 \mu\text{m}$  (hollow symbols). Inset: correlation length as a function of bed height.

where experiments show that  $\xi$  decreases with  $\phi$  (Segre *et al.* 1977; Guazzelli 2001). This suggests that there is an alternative mechanism that sets the scale of  $\xi$ .

To elucidate this new mechanism, we first test whether the magnitude of the fluctuations is set by the same balance between Poisson density fluctuations and Stokes drag (Brenner 1999; Hinch 1988; Rouyer *et al.* 2000). We therefore plot  $\Delta v/v_p$  as a function of  $\phi\xi/a$  for four different experiments (figure 5). The very strong correlation is well fitted with an exponent of  $1/2$ .<sup>†</sup> This confirms that the same fluctuation-drag mechanism pertains for fluidized beds as for sedimentation. Note that in figure 5 we divide the  $\phi\xi$  measured at a given location in the cell by the average particle size in the whole cell; the power law is not changed if we instead divide by the local particle size.

What causes the different dependence of  $\xi$  (and hence  $\Delta v$ ) on  $\phi$ ? In sedimentation we have previously argued (Mucha & Brenner 2003; Mucha *et al.* 2004; Tee *et al.* 2002) that the size of the velocity fluctuations is set by the ambient stratification; the rate of decay of statistical fluctuations  $\Delta v/l$  must be smaller than the decay rate of a density perturbation in the background stratification, and this sets a maximum size for the statistical density fluctuations. However, in a stable fluidized bed, the rate of decay of density fluctuations is not directly caused by the density stratification. As we have demonstrated above, the steady-state density stratification itself results from the balance between upflow from the pump and backflow from the particles of different sizes. Therefore any density fluctuation causes an imbalance between these two effects, and the size of this imbalance dictates the decay rate.

We can calculate this decay rate in the low-volume-fraction limit, valid near the top of the fluidized bed. Batchelor demonstrated (Batchelor 1982; Batchelor & Wen

<sup>†</sup> It is perhaps surprising that this scaling is not appreciably affected by other high- $\phi$  effects. However the fact that high volume fraction fluctuations also obey the Poisson fluctuation law was previously discovered by Segrè *et al.* (2001), in the context of high-volume-fraction sedimentation experiments. Extending the Poisson argument to high volume fraction leads to changes in the effective viscosity, settling viscosity and volume exclusion effects. Although each of these individually varies strongly with volume fraction Segrè *et al.* (2001) argued that the product of these factors is relatively constant over the volume fractions covered.

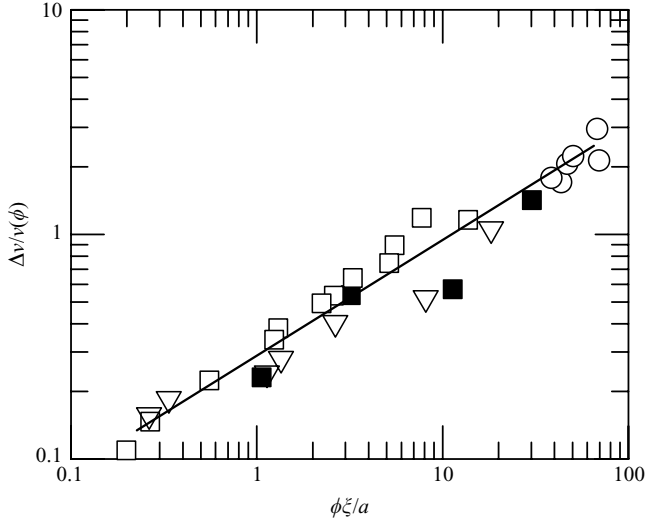


FIGURE 5. Velocity fluctuations as a function of  $\phi\xi/a$  for four different experiments, labelled by radius of particles used in experiments: 57.8  $\mu\text{m}$  (solid squares); 49.0  $\mu\text{m}$  (circles); 68.8  $\mu\text{m}$  and 82.5  $\mu\text{m}$  (open squares); and 49.0  $\mu\text{m}$  and 68.8  $\mu\text{m}$  (inverted triangles). The solid line is a power-law fit, yielding an exponent of  $0.50 \pm 0.02$ .

1982) that the velocity of the  $i$ th species in the presence of the other particles in a dilute polydisperse mixture is given by  $v_{sed,i} = v_{s,i}(1 - 6.55\phi_i - \sum_{j \neq i} S_{ij}\phi_j)$ , where  $v_{s,i}$  is the Stokes velocity of the  $i$ th particles and where the coupling constants,  $S_{ij}$ , depend on the relative sizes and densities of the  $i$ th and  $j$ th particles (Batchelor 1982; Batchelor & Wen 1982). If  $D = \xi \Delta v$  is the particle diffusivity, and  $v_p$  is the velocity of the pump, the time evolution of the volume fraction of the  $i$ th species therefore obeys

$$\frac{\partial \phi_i}{\partial t} + \frac{\partial}{\partial z} \{ \phi_i [v_p - v_{sed}] \} = \frac{\partial}{\partial z} \left[ D \frac{\partial \phi_i}{\partial z} \right]. \quad (1)$$

To compute the decay time constant, we perturb  $\phi_i$  to  $\phi_i + \delta\phi_i$ , and linearize (1), yielding

$$\frac{\partial \delta\phi_i}{\partial t} - \frac{\partial}{\partial z} \left\{ \phi \left. \frac{dv_{sed}}{d\phi} \right|_{\phi} \delta\phi_i \right\} = \frac{\partial}{\partial z} \left[ D \frac{\partial \delta\phi_i}{\partial z} \right]. \quad (2)$$

Now since  $dv_{sed}/d\phi|_{\phi} = C$ , for some constant  $C$ , we can solve (2) with the ansatz

$$\delta\phi_i = A_i \exp\{-t/\tau(k)\} \exp\{i\omega t + ikx\}. \quad (3)$$

The solution is that the decay time  $\tau(k)^{-1} = Dk^2$ , whereas  $\omega \approx C\phi v_s k$  with the prefactor  $C$  depending on the polydispersity of the particle distribution. For monodisperse particles  $C \sim 6.55$  while with the size ratio of the bidisperse experiments we obtain  $C \sim 5.7$ .

Equation (3) therefore demonstrates that density perturbations propagate with velocity  $v_g = d\omega/dk = C\phi v_s$  as they diffuse. Hence a density perturbation advects away with a rate  $v_g/l$ . This rate must be less than the decay rate of the density fluctuation due to diffusion  $D/l^2 = \Delta v/l$ . Hence, the largest density fluctuation must obey  $\Delta v \sim v_g$ . Using  $\Delta v = Fv_o(\phi\xi/a)^{1/2}$  (figure 5) we find a linear dependence,  $\xi/a \sim (C/F)^2\phi$ , consistent with figure 4. Moreover, fitting the prefactor  $F \approx 0.3$  from

figure 5, implies that  $(C/F)^2 a$  is 2.8 cm for the monodisperse particles, and 2.7 cm for the bidisperse particles (taking  $a$  to be the average). This compares reasonably well with the measured slopes in figure 4 of 4.4 cm and 4.0 cm.

To conclude, we have presented the first direct experimental evidence demonstrating that local velocity fluctuations in a fluidized bed are controlled by the balance between locally Poisson density fluctuations and Stokes drag (Caflich & Luke 1985). However, the local correlation length in a fluidized bed increases with volume fraction in striking contrast to sedimentation. We argue that the difference between these two seemingly similar experiments is caused by the different dynamics of small density fluctuations: in the fluidized bed the dynamics is dictated by the balance between the upflow from the pump and the backflow from the particles

This work was supported by NASA (NAG3-2376), the Harvard MRSEC (DMR-0213805), and the NSF Division of Mathematical Sciences (to PJM and MPB).

#### REFERENCES

- ADRIAN, R. J. 1991 Particle-imaging techniques for experimental fluid-mechanics. *Annu. Rev. Fluid Mech.* **23**, 261–304.
- AL-NAAFA, M. A. & SELIM, M. S. 1992 Sedimentation of monodisperse and bidisperse hard-sphere colloidal suspensions. *AIChE J.* **38**, 1618–1630.
- ASMOLOV, E. S. 2004 Evolution of fluctuations in a suspension sedimenting in a container bounded by horizontal walls. *Phys. Fluids* **16**, 3086–3093.
- BARGIEL, M., FORD, R. A. & TORY, E. M. 2005 Simulation of sedimentation of polydisperse suspensions: A particle-based approach. *AIChE J.* **51**, 2457–2468.
- BATCHELOR, G. K. 1982 Sedimentation in a dilute polydisperse system of interacting spheres. Part 1. General theory. *J. Fluid Mech.* **119**, 379–408.
- BATCHELOR, G. K. & WEN, C.-S. 1982 Sedimentation in a polydisperse system. Part 2. *J. Fluid Mech.* **124**, 495–528.
- BERGOUNOUX, L., GHICINI, S., GUAZZELLI, E. & HINCH, J. 2003 Spreading fronts and fluctuations in sedimentation. *Phys. Fluids* **15**, 1875–1887.
- BRENNER, M. P. 1999 Screening mechanisms in sedimentation. *Phys. Fluids* **11**, 754.
- BRUNEAU, D., ANTHORE, R., FEUILLEBOIS, F., AUVRAY, X. & PETIPAS, C. 1990 Measurement of the average velocity of sedimentation in a dilute polydisperse suspension of spheres. *J. Fluid Mech.* **221**, 577–596.
- CAFLISCH, R. E. & LUKE, J. H. C. 1985 Variance in the sedimentation speed of a suspension. *Phys. Fluids* **28**, 759.
- COUDERC, J. P., DAVIDSON, J. F., CLIFT, R. & HARRISON, D. 1985 *Fluidization*. Academic.
- COWAN, M. L., PAGE, J. H. & WEITZ, D. A. 2000 Velocity fluctuations in fluidized suspensions probed by ultrasonic correlation spectroscopy. *Phys. Rev. Lett.* **85**, 453.
- CUNHA, F. R., ABADE, G. C., SOUSA, A. J. & HINCH, E. J. 2002a Modeling and direct simulation of velocity fluctuations and particle-velocity correlations in sedimentation. *Trans. ASME J. Fluids Engng* **124**, 957–968.
- CUNHA, F. R., SOUSA, A. J. & HINCH, E. J. 2002b Numerical simulation of velocity fluctuations and dispersion of sedimentating particles. *Chem. Engng Commun.* **189**, 1105–1129.
- DAVIES, R. 1968 The experimental study of the differential settling of particles in suspension at high concentration. *Powder Tech.* **2**, 43.
- GUAZZELLI, E. 2001 Evolution of particle-velocity correlations in sedimentation. *Phys. Fluids* **13**, 1537.
- HAM, J. M. & HOMSY, G. M. 1988 Hindered settling and hydrodynamic dispersion in quiescent sedimenting suspensions. *Intl J. Multiphase Flow* **14**, 533.
- HINCH, E. J. 1988 Sedimentation of small particles. In *Disorder and Mixing* (ed. E. Guyon, J.-P. Nadal & Y. Pomeau), p. 153–161. Kluwer.
- HOYOS, M., BACRI, J. C., MARTIN, J. & SALIN, D. 1994 A study of the sedimentation of noncolloidal bidisperse, concentrated suspensions by an acoustic technique. *Phys. Fluids* **6**, 3809–3817.

- KUUSELA, E., LAHTINEN, J. M. & ALA-NISSILA, T. 2003 Collective effects in settling of spheroids under steady-state sedimentation. *Phys. Rev. Lett.* **90**, 094502.
- KUUSELA, E., LAHTINEN, J. M. & ALA-NISSILA, T. 2004 Sedimentation dynamics of spherical particles in confined geometries. *Phys. Rev. E* **69**, 066310.
- LOCKETT, M. J. & ALHABBOO, H. M. 1973 Differential settling by size of 2 particle species in a liquid. *Trans. Inst. Chem. Engrs* **51**, 281–292.
- MARTIN, J., RAKOTOMALALA, N. & SALIN, D. 1995 Hydrodynamic dispersion of noncolloidal suspensions - measurement from Einsteins argument. *Phys. Rev. Lett.* **74**, 1347–1350.
- MIRZA, S. & RICHARDSON, J. F. 1979 Sedimentation of Suspensions of Particles of 2 or more Sizes. *chem. Engng Sci.* **34**, 447–454.
- MUCHA, P. J. & BRENNER, M. P. 2003 Diffusivities and front propagation in sedimentation. *Phys. Fluids* **15**, 1305–1313.
- MUCHA, P. J., TEE, S. Y., WEITZ, D. A., SHRAIMAN, B. I. & BRENNER, M. P. 2004 A model for velocity fluctuations in sedimentation. *J. Fluid Mech.* **501**, 71–104.
- NGUYEN, N. Q. & LADD, A. J. C. 2005 Sedimentation of hard-sphere suspensions at low Reynolds number. *J. Fluid Mech.* **525**, 73–104.
- NICOLAI, H. & GUAZZELLI, E. 1995 Effect of the vessel size on the hydrodynamic diffusion of sedimenting spheres. *Phys. Fluids* **7**, 3.
- PAGE, J. H., COWAN, M. L. & WEITZ, D. A. 2000 Diffusing acoustic wave spectroscopy of fluidized suspensions. *Physica B* **279**, 130.
- RAFFEL, M. 1998 *Particle Image Velocimetry*. Springer.
- ROUYER, F., LHUILLIER, D., MARTIN, J. & SALIN, D. 2000 Structure, density, and velocity fluctuations in quasi-two-dimensional non-Brownian suspensions of spheres. *Phys. Fluids* **12**, 958–963.
- SEGRÈ, P. N. 2002 Origin of stability in sedimentation. *Phys. Rev. Lett.* **89**.
- SEGRÈ, P. N., HERBOLZHEIMER, E. & CHAIKIN, P. M. 1997 Long-range correlations in sedimentation. *Phys. Rev. Lett.* **79**, 2574.
- SEGRÈ, P. N., LIU, F., UMBANHOWAR, P. & WEITZ, D. A. 2001 An effective gravitational temperature for sedimentation. *Nature* **409**, 594.
- SEGRÈ, P. N. & MCCLYMER, J. P. 2004 Fluctuations, stratification and stability in a liquid fluidized bed at low Reynolds number. *J. Phys. Condensed Matter* **16**, S4219–S4230.
- SELIM, M. S., KOTHARI, A. C. & TURIAN, R. M. 1983 Sedimentation of multisized particles in concentrated suspensions. *AIChE J.* **29**, 1029–1038.
- SMITH, T. N. 1965 Differential sedimentation of particles of 2 different species. *Trans. Inst. Chem. Engrs and The Chem. Engr* **43**, T69.
- SMITH, T. N. 1966 Sedimentation of particles having a dispersion of sizes. *Trans. Inst. Chem. Engrs and The Chem. Engr* **44**, T153.
- SMITH, T. N. 1967 Differential sedimentation of particles of various species. *Trans. Inst. Chem. Engrs and The Chem. Engr* **45**, T311.
- TEE, S. Y., MUCHA, P. J., CIPELLETTI, L., MANLEY, S., BRENNER, M. P., SEGRÈ, P. N. & WEITZ, D. A. 2002 Nonuniversal velocity fluctuations of sedimenting particles. *Phys. Rev. Lett.* **89**, 054501.
- XUE, J.-Z., HERBOLZHEIMER, E., RUTGERS, M. A., RUSSEL, W. B. & CHAIKIN, P. M. 1992 Diffusion, dispersion, and settling of hard spheres. *Phys. Rev. Lett.* **69**, 1715.